Scalable Computing: Practice and Experience, ISSN 1895-1767, http://www.scpe.org
© 2024 SCPE. Volume 25, Issues 3, pp. 2034–2047, DOI 10.12694/scpe.v25i3.2701

PRODUCT DESIGN FOR THE ELDERLY BASED ON HUMAN-COMPUTER INTERACTION IN THE ERA OF BIG DATA

ZHIHONG LIU*

Abstract. Since 21st century, social aging trend has become more and more serious. It needs accurately identify the nursing needs of elderly disabled people, who are characterized by inconvenient movement and unclear speech. How to solve these problems has become a key point in the field of elderly care and medical care. In response to this problem, this research has designed a human-computer interactive gesture recognition system for elderly nursing beds in the context of big data. The recognition rate of the fusion feature + support vector machine (SVM) classifier adopted in this study is higher than 90% for each category of gesture. On the test set, this method has an average recognition rate of 96.35%, which is much higher than that of single feature + SVM classifier. While other methods' recognition rate is lower than 90%. The recognition rate of tag c (nursing bed posture turning left) with obvious gesture feature information is as high as 99.28%, and that of tag h (nursing bed posture bedpan lowering) with weak gesture feature is 93.65%. The human-computer interaction system has well realized the recognition intention of user's dynamic and static gestures, achieved the goal set by the research, and the interaction form is natural and reliable. In the later research, we can further realize a more comprehensive, accurate and natural human-computer interaction product design through the multi-channel joint decision-making scheme to meet the needs of the elderly.

Key words: Gesture recognition; Human-computer interaction; SVM algorithm; DTW algorithm; Feature fusion

1. Introduction. Since the 21st century, aging trend has become more and more serious in our country. By the end of 2017, the population aged 60 and over was 158 million and 241 million, respectively. That are accounting for 11.4% and 17.3% of the total population, both are 0.6 percentage points higher than 2016 [1-3]. The proportion of the elderly aged 60 and above in the total population in China has exceeded 10%, and has entered into serious aging. At the same time, the problem of population aging is increasingly obvious. Elderly people aged 80 and above in China are increasing at a rate of 5% every year, and will reach 74 and more million by 2040 [4]. The accelerated process of population aging and aging has led to an increasing number of "disabled elderly" who have lost their ability to take care of themselves and "mentally retarded elderly" who have lost their ability to speak clearly and memory decline. According to the latest data of the National Bureau of Statistics, the number of disabled and partially disabled people has exceeded 40 million, and the number of completely disabled people accounts for nearly 30% [5]. Because the elderly with "disability and dementia" have the characteristics of lisping and inconvenient to get up, they not only often need 24-hour care, food, drink and live carefully, but also need to accurately identify the needs of such elderly people, improve their quality of life while maintaining their dignity. The care of such elderly people has become the biggest "pain point" in the field of elderly care and medical care in China, It will bring a severe test to the social old-age medical system. With the significant improvement of computer computing ability, gesture recognition technology has made a major breakthrough in algorithm theory and become an important breakthrough to solve the above problems. To this end, based on the research of gesture recognition algorithm, according to the gesture behavior habits of the elderly disabled, volunteers set up a self-defined sample library, and designed a gesture recognition human-computer interaction system with nursing bed as the carrier. In this study, a human-computer interactive gesture recognition system for the elderly nursing bed was specifically designed on the basis of human-computer interactive product design for the elderly under the background of big data.

2. Related work. Due to the increasingly severe aging trend in our country, the number of "disabled elderly" who have lost the ability to take care of themselves and "mentally retarded elderly" who have lost their

*Ecological Livable College, Hunan Polytechnic of Environment and Biology, Hengyang, 421005, China (Zhihong_Liu2023@outlook.com

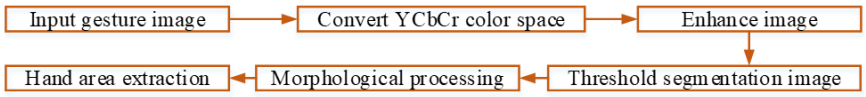

Fig. 3.1: Composition block diagram of hand area pretreatment

ability to speak clearly and memory decline is increasing. And other key issues that need to be solved urgently in the field of elderly care and medical care [6]. Nursing bed control system and human-computer interactive elderly nursing bed gesture recognition system [7]. Foreign gesture recognition technology developed earlier [8]. Mahmoud R et al. used depth optical flow estimation to calculate isolated gestures speed, and extracted relevant features from them. They input it into the linear SVM equally with the constructed gray sequence to achieve the classification of isolation segments. This model had good recall rate and robustness, and good performance and applicability [9]. Pan et al. proposed a hybrid flexible wearable system that can recognize complex gestures. The system used a simple dual-mode capacitive sensor algorithm to develop a low-power interface circuit. The dual-mode sensing platform could simultaneously perceive the space environment and identify local interactions [10]. Miao et al. proposed a new method for dynamic gesture recognition. The gesture recognition accuracy is higher than the existing methods [11]. Zhang et al. proposed a gesture recognition method. This method is based on unsupervised driving. It enabled the transfer of data without data label [12]. Liu et al. proposed a gesture recognition method, which could provide tactile and visual information and simulate neural morphology processing capabilities. This method could carry out 1000 tensile cycles and show excellent tensile endurance while maintaining the stability of electrical properties [13].

Hafsa et al. proposed a improved genetic algorithm (GA). By using non-blind search methods, this model could achieve image reconstruction. This model could use CNN for classification and achieve 92% accuracy [14]. Assisted by deep learning method, Yang J et al. proposed a wearable tactile sensor, which could realize gesture recognition and interaction. Experiments showed that this method could effectively balance the prediction accuracy of the model [15]. To sum up, many mathematicians' research on the design of gesture recognition model can provide reference for this study.

3. Human-computer interaction-based gesture recognition method for the elderly disabled.

3.1. Vision-based gesture image preprocessing method. As aging continues to deepen, it is particularly important to design intelligent elderly products, such as nursing beds and other intelligent medical products. Based on the human-computer interaction of the nursing bed, most elderly disabled people lie or sit on the bed. The complex and changeable background environment will inevitably affect the extraction of gesture target area. Therefore, pre-processing is carried out for collected information image. The block diagram of specific steps is displayed in Figure 3.1.

After the RGB color picture of the collected image is transformed into YCbCr space, the image is enhanced in Figure 1. Then, the single Gaussian model skin color model is used to complete the hand gesture segmentation. Then, the segmented binary image is processed with the morphology of closing first and then opening. The skin-like region is filtered by the area operator. Finally, the hand region obtained by the face elimination algorithm is used for the region graph with only the hand face. The YCbCr color space is derived from YUV (brightness - Y, chroma - U, concentration - V), which can describe digital video signals and optimize the transmission of video or pictures. Formula (3.1) shows the conversion formula from RGB to YCbCr color space.

$$\begin{bmatrix} Y \\ Cb \\ Cr \end{bmatrix} = \begin{bmatrix} 16 \\ 128 \\ 128 \end{bmatrix} + \begin{bmatrix} 65.481 & 128.553 & 24.996 \\ -37.797 & -74.203 & 112.000 \\ 112.000 & -93.786 & -18.214 \end{bmatrix} \begin{bmatrix} R \\ G \\ B \end{bmatrix} \tag{3.1}$$

In the YCbCr color space, the single component Y is the brightness in formula (3.1). Cr and Cb are two color difference components, which are obtained by U and V through a little adjustment and used to store color information. Cb is the difference between the blue component and the reference value. Cr is the difference between the red component and the reference value. And YCbCr occupies less bandwidth. To achieve the best

effect of image preprocessing. Based on the skin color details, the image data of Cr channel is concentrated on the image data of Cr channel, so the image data of Cr channel is taken as the test object in the image of color channel separation. Then the image is smoothed and sharpened to enhance the image. The gesture after image recognition is separated from the face in image segmentation. Otsu dynamic adaptive threshold method is selected for image segmentation. First, set all gray levels in the image as L levels, and the other gray level is the number of pixels. See formula (3.2) for the expression.

$$N = \sum_{i=0}^{L-1} n_i, P_i = \frac{n_i}{N}, \sum_{i=0}^{L-1} P_i = 1 \tag{3.2}$$

The total number of all pixels in the image is N, and the probability of each gray level is P_i in formula (3.2). Then the gray level is divided by the threshold K, and the probability and average gray value of the two groups of gray levels $C_0 = [0, 1, ..., k-1]$ and $C_1 = [k, k+1, ..., L-1]$ the average gray value of the whole image can be obtained, as shown in formula (3.3).

$$\begin{cases} \omega_0 = \sum_{i=0}^{k-1} P_i = \sum_{i=0}^{k-1} n_i \Big/ N, \omega_1 = \sum_{i=k}^{L-1} P_i = \sum_{i=k}^{L-1} n_i \Big/ N = 1 - \omega_0 \\ \mu_0 = \sum_{i=0}^{k-1} iP_i \Big/ \omega_0, \mu_1 = \sum_{i=k}^{L-1} iP_i \Big/ \omega_1 \\ \mu = \sum_{i=0}^{L-1} iP_i = \omega_0\mu_0 + \omega_1\mu_1 \end{cases} \tag{3.3}$$

In formula (3.3), ω_0 is the probability of gray level generation, μ_0 is the average gray value, and μ is the average gray value of the entire image. The average variances of the two groups of C_0 and C_1 are shown in formula (3.4).

$$\sigma_B^2 = \omega_0(\mu_0 - \mu)^2 + \omega_1(\mu_1 - \mu)^2 = \omega_0\omega_1(\mu_1 - \mu_0)^2 = (\mu_1 - \mu)(\mu - \mu_0) \tag{3.4}$$

In formula (3.4), σ_B^2 is the variance between the two groups of gray levels. When inter-class variance owns the largest value, the corresponding optimal threshold is expressed by formula (3.5).

$$k^* = Arg \underset{0 \le i \le L-1}{Max} \left[\sigma_B^2\right] \tag{3.5}$$

After obtaining the optimal threshold k^* in formula (3.5), this method is improved to get better adaptability. At the same time, it is necessary to ensure that the pixel mean distance between the target image and the whole image is $|\mu_0 - \mu|$. The pixel mean distance between the background image and the whole image is $|\mu_1 - \mu|$ as large as possible. Only when the above conditions are met can the weighted sum or product of the two be maximized. According to this idea, the pixel average variance is used to replace the pixel average. In formula (3.6), the improved new threshold formula is shown.

$$k^* = Arg \underset{0 \le i \le L-1}{Max} \left[\left(\sigma_0^2 - \sigma^2\right)^2 \left(\sigma_1^2 - \sigma^2\right)^2\right] \tag{3.6}$$

The improved new threshold has certain robustness to the impact of image contrast and brightness changes in formula (3.6). However, there are still burrs, holes and object noise in the binary image. Mathematical morphological transformation can eliminate noise and elements irrelevant to the image itself. Including corrosion, expansion and opening and closing operations. Suppose A is the target area on the (x, y) plane, S is the structural element with the size and shape set, and the corresponding area of the structural element S on this coordinate is $S(x, y)$. In formula (3.7), the results of corrosion, expansion and opening and closing operations in A zone are shown.

$$\begin{cases} (x, y) \,|(x, y) \in A, S(x, y)/A = \emptyset \\ (x, y) \,|(x, y) \in A, S(x, y) \cap A \neq \emptyset \\ A \circ S = (A - S) + S \\ A \bullet S = (A + S) - S \end{cases} \tag{3.7}$$

Fig. 3.2: Area operator operation and face detection elimination diagram

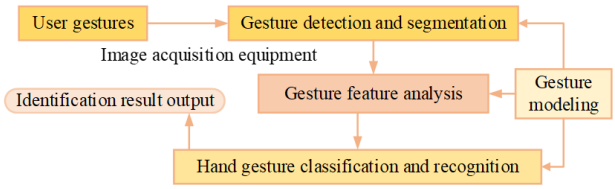

Fig. 3.3: Gesture recognition process

In formula (3.7), S is the structural element. First, in terms of corrosion, move from the upper left corner of the image in order. When S moves to a coordinate point and S is in the target area. The pixel points will be retained, otherwise deleted. Secondly, in terms of expansion, move the position of S from the top left corner of the image in sequence. When S moves to a coordinate point and the area of S and the target image intersect, it will be retained, otherwise it will be deleted. In the open and close operation, $A + S$ is the expansion of S pair. $A - S$ is the corrosion of S pair A, so A is defined as the open operation of S pair A. $A \bullet S$ is the closed operation that S does to A. Then, in Figure 3.2, the area operator is used to filter the specific effect.

First remove the non-skinned areas in Figure 3.2. Secondly, the face detection file method of OpenCV is used to draw ellipse for the face area detected by Cascade Classifier. Finally, the area operator is used to detect the face and eliminate the final effect.

3.2. Dynamic and static gesture feature extraction and recognition methods. In terms of dynamic and static gesture extraction, static gesture feature extraction is based on hand shape change, mainly using physical, geometric and mathematical features [16]. Dynamic gesture feature extraction is mainly through tracking the moving target, and the tracking algorithm obtains the track feature of the gesture area to recognize the gesture. Finally, the fusion of dynamic and static gesture features is realized. Figure 3.3 shows the overall process of gesture recognition.

First of all, on the extraction of static gestures, Fourier descriptor gesture contour extraction. Gesture structure feature extraction based on the ratio of perimeter to area of gesture contour. In formula (3.8), the perimeter of the gesture is calculated by the sum of the closed curve pixel points in the gesture contour area.

$$C = \sum \sum n(x, y) \tag{3.8}$$

In formula (3.8), C is the perimeter of the gesture contour. The pixel on the contour curve is 255. Calculate the number of white pixel points in all areas in the figure to get C. In formula (3.9), $n(x, y)$ is the number of white pixels on the contour.

$$n(x, y) = \begin{cases} 1 & ,if\ f(x, y) = 255 \\ 0 & ,others\ f(x, y) = 0 \end{cases} \tag{3.9}$$

In formula (3.9), $f(x, y)$ is the pixel value corresponding to point (x, y). Therefore, the processed image is always a binary image with 255 or 0 pixels. Scan the binary image of the gesture area. Formula (3.10) is the formula for calculating the area in the gesture contour area.

$$S = \sum \sum N(x, y) \tag{3.10}$$

In formula (3.10), $N(x, y)$ is the number of white pixels in the contour closed area, and the calculation formula of $n(x, y)$ is the same. The calculation of specific gesture area perimeter ratio M is shown in formula (3.11).

$$M = S/C \tag{3.11}$$

The final gesture area and perimeter ratio can be calculated by formula (3.11). The obtained gesture binary sample is as shown in Figure 3.2(c), and the size is uniformly adjusted to 320 * 240 resolution. Dynamic gesture feature extraction is carried out by using the hand gesture centroid of the track tracking algorithm Cam shift and the dynamic object of the optical flow method. Cam shift algorithm is a continuous adaptive Mean Shift tracking algorithm. In formula (3.12), Mean Shift tracking algorithm determines the zero-order moment M_{00}, first-order moment M_{01}, M_{10} and second-order moment M_{20}, M_{02}, M_{11} of the target color probability distribution.

$$\begin{cases} M_{00} = \sum_x \sum_y I(x, y) \\ M_{01} = \sum_x \sum_y xI(x, y) \\ M_{10} = \sum_x \sum_y yI(x, y) \\ M_{20} = \sum_x \sum_y x^2 I(x, y) \\ M_{02} = \sum_x \sum_y y^2 I(x, y) \\ M_{11} = \sum_x \sum_y xyI(x, y) \end{cases} \tag{3.12}$$

According to formula (3.12), we can get the centroid position (x, y). Formula (3.13) represents the bearing angle θ with the target.

$$\begin{cases} (x, y) = (M_{10}/M_{00}, M_{01}/M_{00}) \\ \theta = 1/2 \arctan \left[2(M_{11}/M_{00} - xy) / (M_{20}/M_{00} - x^2) - (M_{02}/M_{00} - y^2) \right] \end{cases} \tag{3.13}$$

After the centroid position is obtained in formula (3.13), it is necessary to judge whether the center position coordinate at this time has reached convergence. If not, return to the step of formula (3.12) and recalculate the area. The characteristics of gesture motion track mainly include: position information, speed and direction angle. Formula (3.14) is the expression formula of the trajectory direction angle of the gesture centroid.

$$\theta_t = \arctan \left[(y_t - y_{t-1}) / (x_t - x_{t-1}) \right] \tag{3.14}$$

In formula (3.14), θ_t and (x_t, y_t) are the azimuth and position coordinates at time t. (x_{t-1}, y_{t-1}) is its position coordinate at the time of Dt-1. Dynamic gesture feature extraction based on optical flow method. LK optical flow algorithm is not only fast in operation, but also accurate in tracking target. The image pyramid is a sequence of images with scale changes obtained from a group of adjacent level images through a previous low-pass filter. Assume that the abscissa value of the image element is x, y is the ordinate value. Formula (3.15) is the inter-layer operation.

$$G_i(x, y) = \sum_{m=-2}^{2} \sum_{n=-2}^{2} w(m, n) G_{i-1}(2x + m, 2y + n) \tag{3.15}$$

The lowest layer G_0 of the image is the original image, and G_i is the image of layer i in formula (3.15). The pixels of layer i are obtained by weighted average of the image matrix corresponding to the previous layer

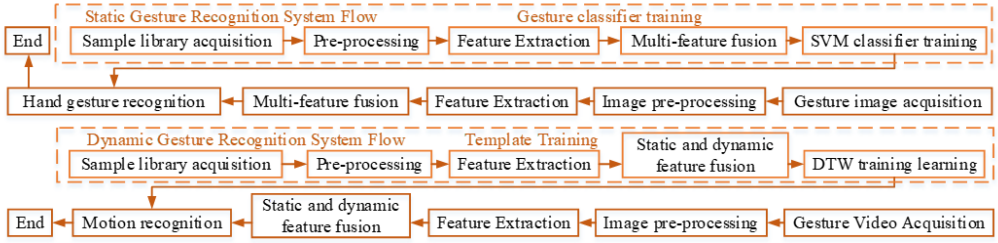

Fig. 3.4: Dynamic and static gesture recognition system flow

through Gaussian window function w. $w(m,n)$ is the window function. When the window size is 5 * 5, the four constraints in equation (3.16) are met.

$$\begin{cases} w(m,n) = w(m) * w(n), m \in [-2,2], n \in [-2,2] \\ \sum_{-2}^{2} w(m) = 1 \\ w(m) = w(-m) \\ w(-2) + w(2) + w(0) = w(-1) + w(1) \end{cases} \tag{3.16}$$

The window function can be obtained by equation (3.16). In the method of hand gesture target classification, we mainly adopt (dynamic) template matching method and (static) support vector machine method. Figure 4 describes the flow chart of dynamic and static gesture recognition system.

In the recognition of static gestures, the training set uses SVM classifier for parameter adjustment training in Figure 3.4. In the recognition of dynamic gestures, DTM algorithm is used to compare the obtained hand shape and trajectory fusion feature vectors with the training samples in the template library. The gesture with the shortest matching distance is the gesture to be recognized. Equation (3.17) describes the linear mapping function expression of specific SVM.

$$f(x_i, w, b) = w^T x_i - b \tag{3.17}$$

In formula (3.17), the penalty function $f(x_i, w, b)$ is defined as the scoring function of SVM. w^T and b are the parameters that SVM needs to train. There are 8 kinds of gestures to distinguish. Because the sample type is not large, the "one-to-one" multi-classification strategy is selected, which can ensure high accuracy and will not cause too much loss in speed. The final decision function of "one-to-one" multi-classification is expressed by formula (3.18).

$$\begin{cases} y = \arg \max\limits_{i \in [1,2,\ldots,n]} \left(\sum_{j \neq i} count_{ij} \right) \\ count_{ij} = \begin{bmatrix} 1 & SVM_{ij}(x) \to i \\ 0 & SVM_{ij}(x) \to j \end{bmatrix} \end{cases} \tag{3.18}$$

In formula (3.18), the SVM classifier decision samples composed of $SVM_{ij} \to i$ and j belong to class i. For 8 different types of gestures, 28 SVM classifiers need to be constructed, and the decision function is used to determine which type of gesture to be recognized is the closest among the 8 gesture categories. In the training stage of SVM, it is still necessary to manually input some super parameters. The change of decision function after the introduction of kernel function is shown in formula (3.19).

$$f(x) = sgn \sum_{i-1}^{n} a_i * y_i K(x_i *, x) + b* \tag{3.19}$$

The RBF kernel function is selected to map the samples to the high-dimensional space in formula (3.19), so better training and classification results can be obtained. The optimization of dynamic gesture recognition

is using DTW algorithm. The global optimal path of the DTW algorithm is only related to the region within the parallelogram, and the feature vector sequence to be recognized does not need to consider the element matching outside the region. The dynamic path is divided into three parts $(1, X_a)$, (X_{a+1}, X_b) and (X_{b+1}, N). In Formula (3.20), through the slope of the parallelogram, the values of D and E can be calculated.

$$\begin{cases} X_a = 1/3(2M - N) \\ X_b = 2/3(2N - M) \end{cases} \tag{3.20}$$

In formula (3.20), the length condition of M, N is limited by $2M - N \geq 3$ hand $2N - M \geq 2$. In this constraint, each frame on the i axis only needs to be compared with the frame between $[y_{\min}, y_{\max}]$ on the j axis. When $X_a = X_b$, the comparison is divided into two sections. See Formula (3.21) for details.

$$\begin{cases} 1/2x \sim 2x, & x \leq x_a \\ 2x + (M - 2N) \sim 1/2x + (M - 1/2N), & x > x_b \end{cases} \tag{3.21}$$

When $X_a < X_b$, the comparison is divided into three sections. See formula (3.22) for details.

$$\begin{cases} 1/2x \sim 2x, & x \leq x_a \\ 1/2x \sim 1/2x + (M - 1/2N), & x_a < x \leq x_b \\ 2x + (M - 2N) \sim 1/2x + (M - 1/2N), & x > x_b \end{cases} \tag{3.22}$$

In the comparison of formula (3.22), when $X_a > X_b$, the situation is similar. In template training and recognition, the matching distance of DTW algorithm is calculated by Euclidean distance. Set the eigenvector of the input unknown gesture value as $X = (x_1, x_2, ..., x_m)$, and the eigenvector of a gesture sample in the template library as $G = (g_1, g_2, ..., g_m)$. See Formula (3.23) for the calculation of specific Euclidean distance.

$$D(X, G) = \sqrt{\sum_{i=1}^{m} (x_i - g_i)^2} \tag{3.23}$$

At the same time, select $\alpha(M + N)$. And α is a positive proportion coefficient, whose value is 0.25.

4. Test and analysis of gesture recognition system for elderly nursing bed based on human-computer interaction.

4.1. Analysis of test results of dynamic and static gesture recognition.. To verify the effectiveness of gesture recognition system for elderly nursing bed based on human-computer interaction. The customized gesture information includes 8 different categories. The software environment of Visual Studio 2015 (community) and OpenCV3.4.00 is adopted. The camera captures video at a frame rate of 30 frames/s. The extracted two-dimensional image has a resolution of 640 * 480. For the "one-to-one" strategy, 28 SVM two-classifiers are constructed and the classification of gestures is determined by voting. The obtained gesture classification results correspond to the command information of a bed posture control respectively in the text, achieving the purpose of human-computer interaction. Tn Figure 4.1, the binary diagram of some samples in the dataset is shown.

The number of gesture values that can be selected in the experiment is 8 in Figure 4.1, and the specific gesture shape can be customized according to the user's actual situation. The final classification of the SVM classifier is obtained from the "one-to-one" voting results of each test image. In order to protect the privacy of users, the collected data was anonymized and encrypted. First, hashing algorithm is used to convert personal identifiable information (such as name, email, mobile phone number) and other data into irreversible anonymous identifiers to achieve data anonymity. Secondly, AES strong encryption algorithm is used to encrypt the whole data set to ensure the security of data in storage and transmission. Finally, assign data access to authorized users or roles, and ensure that only those who need to know specific information can access relevant data. Compare it with the real category of the image and calculate the recognition rate of each gesture category. As shown in Table 4.1 below, the total number of training samples is 8 * 1280, and the number of test samples is 8 * 640.

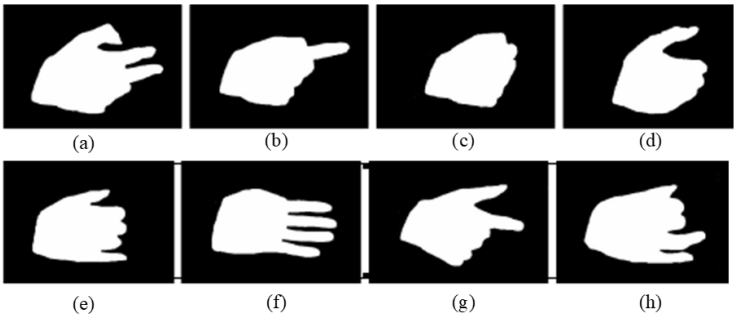

Fig. 4.1: Schematic diagram of binary sample

Table 4.1: Static gesture recognition rate

Gesture label	Recognition rate of training samples	Test sample recognition rate
a	0.9678312	0.9615375
b	0.974025	0.974025
c	0.9928062	0.9865125
d	0.9709281	0.9615375
e	0.9615375	0.9365625
f	0.974025	0.974025
g	0.9865125	0.9615375
h	0.9615375	0.9365625

The recognition rate of fusion feature + SVM classifier for each type of gesture is greater than 90% in Table 1. The recognition rate of tag c with obvious gesture feature information is as high as 99.28%, and that of tag h with weak gesture feature is 93.65%. The specific effect is shown in Figure 4.2 (a). However, advantages and disadvantages' comparison of the fusion feature algorithm is difficult only by the recognition rate of the data set. So the recognition rate test of single feature extraction for the control variables of the data set was conducted. After RGB image preprocessing and gesture segmentation, the sample library of the data set in the previous article is extracted using moment invariants and single features of Fourier descriptors. At the same time, conduct SVM training and testing. Figure 4.2(b) records the comprehensive average recognition rate comparison of 8 * 640 sample test sets of eight gestures.

This fusion feature extraction is very effective in classification and can well achieve static gesture recognition in Figure 4.2. The fusion feature + SVM classifier in this study is comprehensive. On the test set, this method's average recognition rate is 96.35%, which is much higher than that of single feature + SVM classifier. Other methods' recognition rate are lower than 90%. To some extent, it alleviates the problem of low accuracy caused by information waste. In the comparison of dynamic gesture recognition rate, the test set of volunteer gesture video data set is tested. First, four kinds of gestures in 1280 video images are processed frame by frame, then the image area of the gesture is extracted and the optical flow of the two adjacent frames is calculated, and the hand shape is normalized by feature extraction. The trajectory features and fusion features obtained only by pyramid optical flow method are compared and verified. Table 4.2 describes the comparative recognition rate of the two methods.

When faced with the distinction between eating and drinking gestures, the classification effect of static hand shape feature and dynamic track feature fusion is better than that of using dynamic track feature alone in Table 4.2. Figure 4.3 shows the specific effect analysis.

Figure 4.3 shows that less than 60% of gesture recognition optical flow features for eating and drinking, while the recognition rate of fusion features is greater than 80%. The essential reason is that the movement tracks

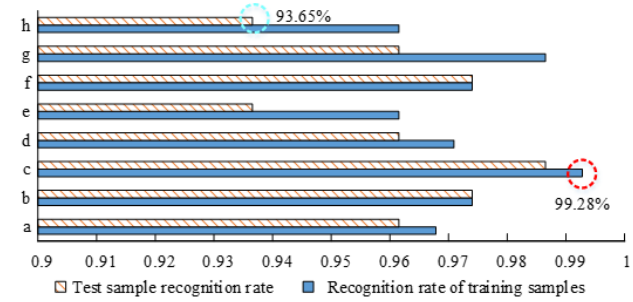

(a) Structural Similarity

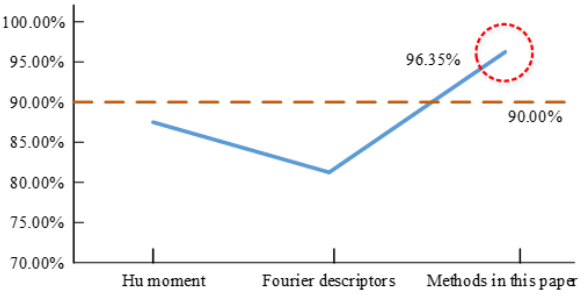

(b) Information Entropy

Fig. 4.2: Static gesture recognition rate

Table 4.2: Dynamic gesture recognition rate

Gestures	Optical flow feature recognition rate	Fusion feature recognition rate
Eating	0.5369625	0.8366625
Drinking water	0.574425	0.8616375
Urination	0.824175	0.8866125
Defecation	0.874125	0.924075

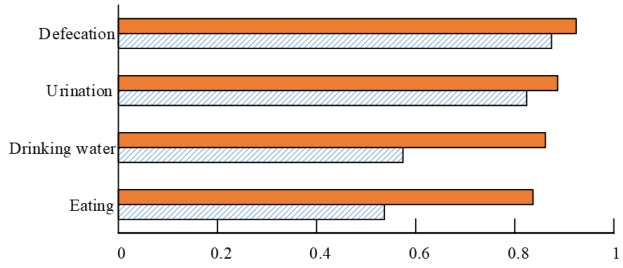

Fig. 4.3: Static gesture recognition rate

Table 4.3: The 8 action command codes correspond to the table

Action Instructions	Hand gestures	Command Code
Backlift	a	0X01
Back Down	b	0X02
Left flip	c	0X03
Right flip	d	0X04
Back up leg bend	e	0X05
Back flat leg extension	f	0X06
Potty up	g	0X07
Potty down	h	0X08

of eating and drinking are quite close, but the hand shape is different, so the individual track characteristics cannot accurately distinguish them.

4.2. Test result analysis of human-computer interactive gesture recognition system for elderly nursing bed. . To better reflect the feasibility of gesture recognition technology, the effect of the system is tested by building a QT interface, and static gestures are used to achieve bed posture control. Dynamic gestures are used to identify basic physiological needs. Through dynamic and static gesture recognition for the elderly with disabilities, the demand results are displayed on the interface to realize the auxiliary nursing effect of human-computer interaction elderly nursing bed. Firstly, a common monocular camera (CMOS sensor) with a maximum frame of 30 FPS is used as the video acquisition hardware device and installed on the inclined top of the nursing bed (fixed on the ceiling) to facilitate the acquisition of video information; Winowds 10 (Enterprise x64) operating system; DDr4 2400Hz (2 * 8GB) memory and Intel (R) Core (TM) i3-8100 CPU @ 3.60GHz CPU. The software is based on OpenCV3.4.0 open-source computer vision library, programmed under the Visual Studio 2015 (Commuity) platform, and the QT programming framework is used to display the interface effect. In Table 4.3, based on the recognition of static gestures, the nursing bed has 8 action commands, and the corresponding relationship is set.

The gesture corresponding to the command code of 0X01-0X08 controls the posture of the nursing bed in Table 4.3. In dynamic gesture recognition, the customized action template is four basic physiological needs. Before analyzing the characteristics of gestures of elderly disabled people, users need to be trained, and the training process is as follows. First of all, a phased training method is adopted in the implementation of training, so that users can gradually start from basic instructions, understand the relationship between various gestures and nursing bed operation, and finally be able to skillfully complete the expression of bed posture control and basic physiological needs. Second, the time from the beginning of the user's exposure to the system to being able to operate independently is recorded, and the user will begin to be able to perform simple operations on the nursing bed, such as back rising or leg bending, after 1-3 hours of training. However, it can take anywhere from a few days to a week for a user to fully master all of the gesture instructions, depending on individual differences such as age, learning ability and sensitivity to gesture movements. Finally, in order to improve the training process and increase adoption by older users, regular return visits will also be conducted to evaluate the effectiveness of the user's application and collect feedback as a reference for subsequent research and system optimization. After the training, the recognition results are presented in the human-computer interface by analyzing the characteristics of gestures of the elderly disabled. Figure 4.4 shows the test results of the static gesture recognition system.

After recognizing the static gestures in Figures 4.4(a) and 4.4(b), the nursing bed completes the gesture actions of turning right (c) and turning left (d) according to the gesture commands. In dynamic gesture recognition, the human-computer interaction of the nursing bed is tested. Testing in real environment can evaluate the adaptability of the system to complex and changing environments. There may be different illumination, noise levels and background interference in places such as nursing homes, so the adaptability of the test system under these conditions is very important for its practical application. In order to evaluate the performance of the system under different environmental factors, the system was tested in a more realistic environment and

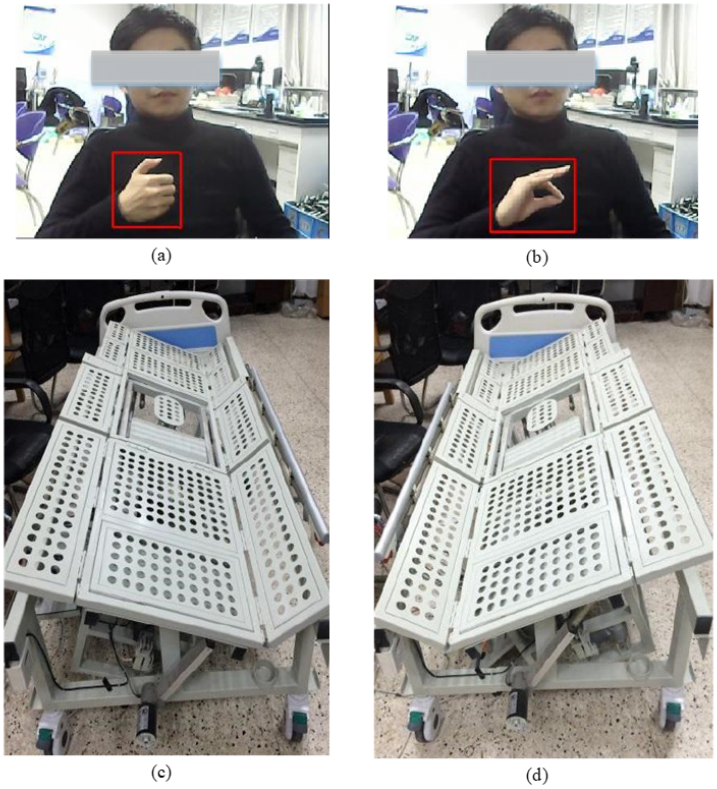

Fig. 4.4: Static gesture recognition test chart

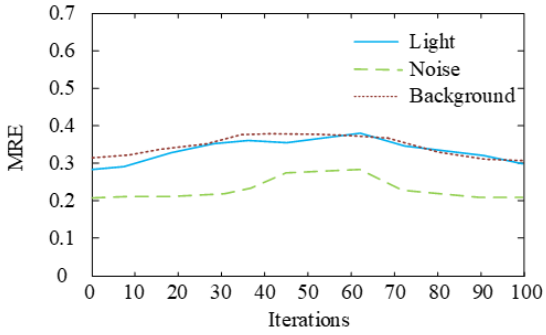

Fig. 4.5: MRE value of the system under different environmental factors

experimented under different environmental conditions. The experimental results are shown in Figure 4.5.

As can be seen from Figure 4.5, the average MRE value of the evaluation system is 0.32 under the interference of lighting environment factors. Under the interference of noise environmental factors, the average MRE value of the evaluation system is 0.25. Under the interference of background interference and environmental factors, the average MRE value of the evaluation system is 0.34. On the whole, the MRE values are all between 0.25 and 0.35, and these smaller values indicate that the prediction results of the evaluation system are close to the real values. The evaluation system performs well under the interference of environmental factors such

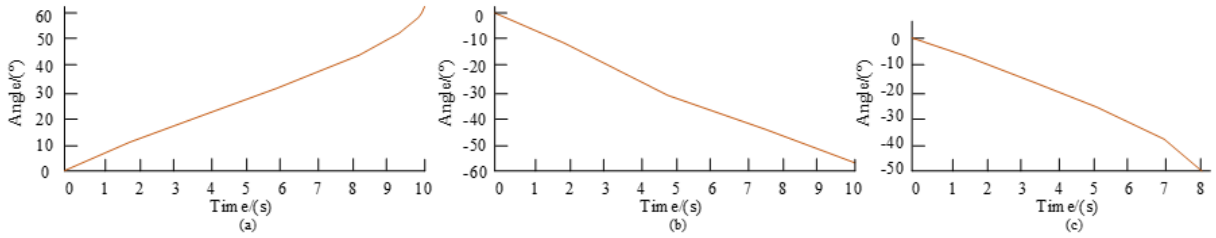

Fig. 4.6: Motion simulation results under dynamic gesture

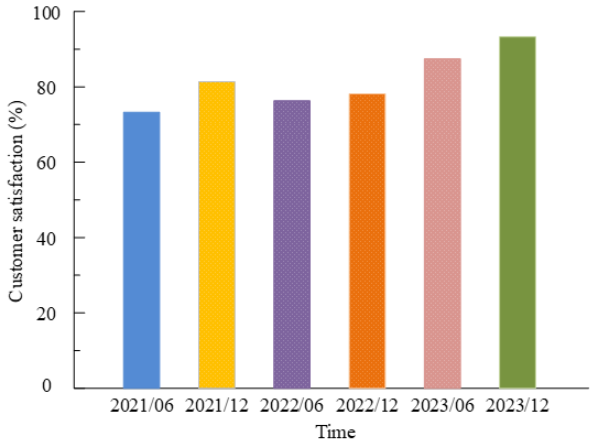

Fig. 4.7: The result chart of user satisfaction survey with time.

as lighting, noise and background interference, and can maintain high accuracy and stability. In Figure 4.6, kinematics simulation is carried out under the action commands of back up, back up, leg bending and left and right turning.

Figure 4.6(a) shows the relationship between time and back lifting angle. The rotation angle of the joint of the back lifting part is 0 ° ∼ 62 °. That meets the design requirements and the angular velocity is relatively gentle, and will not cause secondary injury due to the unstable velocity. That verifies the correctness of the kinematics modeling of the back lifting part of the nursing bed. See Figure 10(b) for the kinematics simulation results of the back-lift leg curve. The joint of the leg bending part can reach an angle of 0 ° ∼ 58 °, and the angular velocity changes smoothly and smoothly, meeting the design requirements of the elderly products. The kinematics simulation results of left and right rolling are shown in Figure 4.6(c). The joint of the rolling part can reach an angle of 0 °∼50 °, and the speed is stable, without obvious speed mutation. The human-computer interaction system has well realized the intention recognition of user's static and dynamic gestures. And it achieved the bed posture control based on static gesture recognition and the demand recognition based on dynamic gestures for users with relatively clear awareness, achieving the goal set by the research, and the interaction form is natural and reliable. User satisfaction can promote the long-term use of nursing bed gesture recognition system by elderly users. To assess the long-term usability of the system, a user satisfaction survey was conducted, the results of which are shown in Figure 4.7.

According to Figure 4.7, in June 2021, the user satisfaction reached 74.52%. This figure rose to 81.49% in December 2021, an increase of 6.97%. However, in June, 2022, user satisfaction dropped to 77.15%, a decrease of 4.34%. However, in December 2022, user satisfaction increased slightly to 78.61%, and in June 2023, it increased significantly to 87.86%. Finally, in December 2023, the user satisfaction reached 92.37%. From the

data analysis, with the passage of time, the overall user satisfaction showed a trend of first rising, then slightly falling, and then continuing to rise. The decrease of satisfaction in the intermediate stage may be caused by the corresponding adjustment of the system. The continuous increase of satisfaction shows that users have a good acceptance and experience of the gesture recognition system. This can not only meet the actual needs of users, but also provide feedback for system developers to improve system functions and performance. This trend reveals that the system has certain attraction and long-term use potential.

5. Conclusion. In view of the increasingly severe trend of social aging in recent years, the number of elderly people with disabilities characterized by lisping and inconvenient movement is increasing. How to meet their nursing needs has become an urgent problem in the field of medical care and old-age care. In response to this problem, this research has designed a gesture recognition system for the elderly nursing bed based on human-computer interaction in the context of big data. The fusion feature + SVM classifier adopted in this study has a recognition rate of more than 90% for each category of gesture. The recognition rate of tag c (nursing bed posture turning left) with obvious gesture feature information is as high as 99.28%, and that of tag h (nursing bed posture bedpan lowering) with weak gesture feature is 93.65%. At the same time, this method can alleviate the problem of low accuracy caused by information waste to a certain extent. The average recognition rate of this method reaches 96.35% on the test set, which is much higher than that of single feature + SVM classifier. While other methods' recognition rate is lower than 90%. Kinematics simulation is carried out under the action command after gesture recognition. The human-computer interaction system can better realize the intention recognition of user's dynamic and static gestures, achieve the expected goal of the research. And the interaction form is natural and reliable. Since older adults may have different physiological and cognitive abilities, future research could examine how the system performs under both ability and physical conditions. The nursing bed gesture recognition system is customized according to the individual needs and wishes of users. In addition to gesture features, consider incorporating other information such as eye tracking, facial expressions, etc., into the system to provide more comprehensive and accurate intent recognition. This enhances the interactivity and user experience of the system.

REFERENCES

[1] Wang, X., Shi, R. & Niu, F. Optimization of furniture configuration for residential living room spaces in quality elderly care communities in Macao. *Frontiers Of Architectural Research*. **11**, 357-373 (2022)
[2] Faba, B., Yecl, A., Tvs, A., Ssm, A., Jt, A., Vs, C., Mg, C., Jdw, C., Ja, C. & Cgc, D. Clinical effectiveness of music interventions for dementia and depression in elderly care (MIDDEL): Australian cohort of an international pragmatic cluster-randomised controlled trial. *The Lancet Healthy Longevity*. **3**, 153-165 (2022)
[3] Mu, Q., Guo, P. & Wang, D. Optimal Subsidy Support for the Provision of Elderly Care Services in China Based on the Evolutionary Game Analysis. *IJERPH*. **19**, 1-20 (2022)
[4] Wang, X., Ma, S., Hu, D., Xu, C., Luo, X. & Tang, Z. Effect of aging temperature on the fatigue properties of shot-peened single crystal superalloy at intermediate temperature. *International Journal Of Fatigue*. **2022**, 6675-10 (0)
[5] Wang, L. Cooperative Elderly Care Services in the Greater Bay Area. *China Report ASEAN*. **7**, 50-52 (2022)
[6] Hu, J., Zhang, Y., Wang, L. & Shi, V. An Evaluation Index System of Basic Elderly Care Services Based on the Perspective of Accessibility. *IJERPH*. **19**, 1-16 (2022)
[7] Trujillo, J., Asli, Z., Kan, C., Irina, S. & Harold, B. Differences in functional brain organization during gesture recognition between autistic and neurotypical individuals. *Social Cognitive And Affective Neuroscience*. **17**, 1021-1034 (2022)
[8] Suni, S. & Gopakumar, K. Extracting Multiple Features for Dynamic Hand Gesture Recognition. *International Journal Of Engineering And Advanced Technology*. **10**, 71-75 (2021)
[9] Mahmoud, R., Belgacem, S. & Omri, M. Towards wide-scale continuous gesture recognition model for in-depth and grayscale input videos. *International Journal Of Machine Learning And Cybernetics*. **12**, 1173-1189 (2021)
[10] Pan, J., Li, Y., Luo Y, Z., Wang, X., Wong, D., Heng, C., Tham, C. & Thean, A. Hybrid-Flexible Bimodal Sensing Wearable Glove System for Complex Hand Gesture Recognition. *ACS Sensors*. **6**, 4156-4166 (2021)
[11] Miao, Y., Li, J. & Sun, S. Dynamic Gesture Recognition Combining Global Gesture Motion and Local Finger Motion. *Journal Of Computer-Aided Design & Computer Graphics*. **32**, 1492-1501 (2020)
[12] Zhang, Y., Wu, L., He, W., Zhang, Z., Yang, C., Wang, Y., Wang, Y., Tian, K., Liao, J. & Yang, Y. An Event-Driven Spatiotemporal Domain Adaptation Method for DVS Gesture Recognition. *IEEE Transactions On Circuits And Systems, II*. **69**, 1332-1336 (2022)
[13] Liu, L., Xu, W., Ni, Y., Xu, Z., Cui, B., Liu, J., Wei, H. & Xu, W. Stretchable Neuromorphic Transistor That Combines Multisensing and Information Processing for Epidermal Gesture Recognition. *ACS Nano*. **16**, 2282-2291 (2022)
[14] Hafsa, M., Atitallah, B., Salah, T., Amara, N. & Kanoun, O. genetic algorithm for image reconstruction in electrical impedance tomography for gesture recognition. *Technisches Messen: Sensoren, Gerate, Systeme*. **89**, 310-327 (2022)

[15] Yang, J., Liu, S., Meng, Y., Xu, W., Liu, S., Jia, L., Chen, G., Qin, Y., Han, M. & Li, X. Self-Powered Tactile Sensor for Gesture Recognition Using Deep Learning Algorithms. *ACS Applied Materials & Interfaces*. **14**, 25629-25637 (2022)
[16] Envelope, M., Rlpdm, B. & Vfdlj, B. Gesture recognition of wrist motion based on wearables sensors. *Procedia Computer Science*. **210**, 181-188 (2022)

Edited by: Zhengyi Chai
Special issue on: Data-Driven Optimization Algorithms for Sustainable and Smart City
Received: Oct 17, 2023
Accepted: Mar 21, 2024